Published in Quaternary International 164-165, 43-52, 2007
which should be used for any reference to this work

First results of cosmogenic dated pre-Last Glaciation erratics from the Montoz area, Jura Mountains, Switzerland

Angela A. Graf[a,*], Stefan Strasky[b], Susan Ivy-Ochs[c], Naki Akçar[a], Peter W. Kubik[d], Martin Burkhard[e,†], Christian Schluchter[a]

[a]*Institute of Geological Sciences, University of Bern, Balzerstrasse 1–3, 3012 Bern, Switzerland*
[b]*Institute of Isotope Geochemistry and Mineral Resources ETHZ, NO CO62.5, Sonneggstrasse 5, 8092 Zürich, Switzerland*
[c]*Institut für Teilchenphysik, ETH Hönggerberg, 8093 Zürich, Switzerland*
[d]*Paul Scherrer Institut c/o Institut für Teilchenphysik, ETH Hönggerberg, 8093 Zürich, Switzerland*
[e]*Institut de Géologie, Rue Emile-Argand 11, CH-2007 Neuchatel, Switzerland*

Abstract

The Jura Mountains are a perialpine chain bending from the SW to the NW of Switzerland. Alpine ice reached only marginal areas of this chain during the Last Glacial Maximum (LGM) but remaining erratic boulders of alpine origin indicate older glaciations of unknown age, tentatively correlated either with the classical Rissian or with the Most Extensive Glaciation. Presented here are the first results of dating these pre-LGM boulders by using cosmogenic radionuclides (^{10}Be) and noble gases (^{21}Ne). Both data sets are in good agreement within 1σ error, with radionuclide apparent exposure ages ranging from 60 to 107 ka, and noble gas apparent ages from 73 to 123 ka. Considering the importance of erosion on older boulders, the age of the erratics corresponds most probably to Marine Isotope Stage 6. These results are encouraging for further studies on pre-LGM erratic boulders in the mid-latitudes.

1. Introduction

The perialpine chain of the Jura Mountains is not only linked to the Alps by their tectonic history (Labhart, 1992), but was also repeatedly influenced by huge ice masses flowing out of the inner-alpine valleys during the Quaternary (Schlüchter, 2004). In comparison to the Alps and the Swiss Midlands, the chronology of the glaciations of this area is poorly constrained, as dating is only available for deposits of the Last Glacial Maximum (LGM) (Buoncristiani and Campy, 2004a; Vannières et al., 2004; Heiri and Millet, 2005). However, relict glacial deposits, e.g. erratic boulders of alpine origin, are found beyond the LGM ice extent. Without age control, these deposits have tentatively been attributed to either the classical Rissian of Penck and Brückner (1901–1909) or to the Most Extensive Glaciation (MEG), thought to be older than 700 ka (Schlüchter and Kelly, 2001).

In view of the need to establish an absolutely dated glacial chronology for the Jura Mountains we have used in situ produced cosmogenic nuclides to date surfaces of erratic boulders found on the top of the Montoz anticline. This area lies beyond the extent of the LGM and is thus appropriate to test Surface Exposure Dating (SED) methods on old erratic boulders. Cosmogenic nuclides are produced in the upper few centimeters of a rock surface as a function of exposure time to cosmic rays. By using both radionuclide ^{10}Be and noble gas ^{21}Ne, it is possible to rule out pre-exposure, which results in an overestimation of the true deposition age. When a surface is covered, ^{10}Be starts to decay while ^{21}Ne is stable, and so each would produce different ages. ^{10}Be and ^{21}Ne dating studies have previously been carried out to cross-check exposure ages in Antarctica (Oberholzer et al., 2000, 2003), Tibet (Schäfer et al., 2002) and the Swiss Midlands (Ivy-Ochs et al., 2004).

* Corresponding author. Fax: +41 31 631 48 43.
E-mail address: angela.graf@geo.unibe.ch (A.A. Graf).
† Deceased in August 2006.

2. Evidence for glaciation of the Jura Mountains

At the southern slope of the first Jura Mountain anticline, e.g. Mont Suchet and Mont Tendre, some 50 km from the outlet of the Rhone valley, the LGM alpine ice of the Rhone glacier reached an altitude of at least 1200 m a.s.l. (Jäckli, 1962). From this point, the Rhone ice body splits into two lobes sloping down to 400 m a.s.l. to the SW of Geneva and to 600 m a.s.l. to the NE of Solothurn (Fig. 1). However, erratic boulders of quite fresh appearance are found at higher altitudes (1395 m a.s.l on Mt d'Amin, W of Chasseral) and far over the Doubs River to the Loue valley near Ornans, France (cf. Hantke, 1978). These boulders clearly indicate that a higher and much more extensive glaciation has overridden most of the Jura Mountains, including high plateaus (> 1000 m a.s.l) such as the Franches Montagnes (Vuille, 1965). The snowline of this "larger than LGM" glaciation dropped down to 700–800 m a.s.l. (Nussbaum and Gygax, 1935; Trümpy, 1980).

The ice extent within the *western* Jura (mainly France) is relatively well constrained, as fronts of the pre-LGM glaciation, the so-called "external moraine complex", extends from Ornans to Bourg-en-Bresse and reached Lyon, where the ice lobe descended to 300 m a.s.l. (Nussbaum and Gygax, 1935; Hantke, 1978; Penck and Brückner, 1901–1909; Campy and Arn, 1991; Campy, 1992; Buoncristiani and Campy, 2004b). On the other hand, the LGM "internal moraine complex" can be followed around 10–40 km inwards of the former extent over more than 100 km length. North of Pontarlier, the ice reached an altitude of 850–950 m a.s.l (Campy and Arn, 1991) and about 550 m a.s.l to the west of Champagnole. It extended to Bourg-en-Bresse (Moscariello et al., 1998), and ended some 20 km before Lyon.

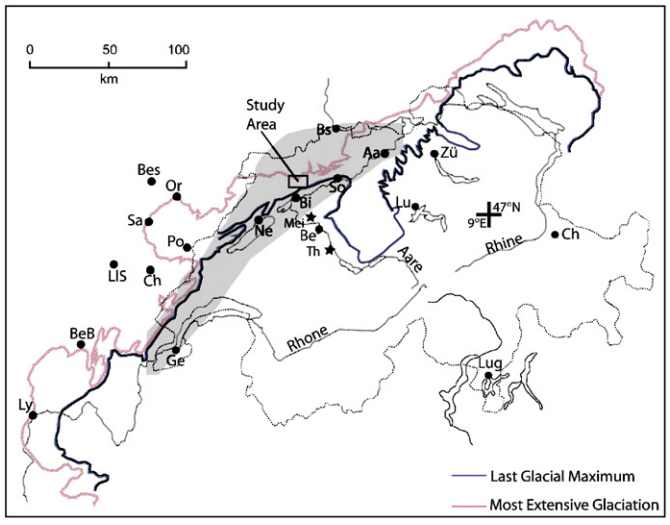

Fig. 1. Extension of the LGM and the MEG in Switzerland (outline shown) and France. The study area is indicated northeast of Biel. The shadowed field corresponds to the extent of Fig. 2 (from Genève to Basel). Aa: Aarau; Beb: Bourg-en-Bresse; Bes: Besançon; Be: Bern; Bi: Biel; Bs: Basel; Cha: Champagnole; Ch: Chur; Ge: Genève; LIS: Lons-le-Saunier; Lug: Lugano; Ly: Lyon; Mei: Meikirch; Ne: Neuchâtel; Or: Orbe; Sa: Salins-les-Bains; So: Solothurn; Th: Tahlgut; Zü: Zürich.

Agassiz (1843) and later Nussbaum and Gygax (1935) defined out a local ice cap covering the *central* part of the Jura Mountain chain, further complicating the reconstruction of glacial chronology. Recent studies by Aubert (1938, 1965), Arn and Aubert (1984), Campy (1992), Badoux (1995) and Buoncristiani and Campy (2004a, b) tend to constrain the extent of this local ice cap during the last two glaciations. They mostly argue on the lodgement till distribution outcropping along the southernmost slope of the central Jura Mountains, where lodgement tills containing exclusively limestones clast from the Jura Mountains are found over the Alpine lodgement tills. From this, as well as from striaes indicating ice flow direction, the above mentioned authors conclude that local ice accumulated in the Joux Valley (Fig. 2), filling up the depression and finally overflowing the passes north- and southward, preventing the alpine Rhone glacier from penetrating most of the central Jura Mountains. During the LGM, local ice extended to the NE into the Vallorbe and Vaulion Valleys (leaving Dent de Vaulion as a nunatack) and to the North (reaching Pontarlier). It is more difficult to constrain the ice cap during the pre-LGM glaciation, but the absence of any alpine material in the "external moraine complex" suggests that both thickness and extension of the ice were larger, and that it culminated at around 2000 m a.s.l. (Campy, 1992).

The *eastern* part of the Jura Mountains (East of the decrochement Vallorbe-Pontarlier) is characterized by generally lower elevation. This, and the absence of an extended local ice sheet allowed the pre-LGM Rhone glacier to penetrate deeper into the ranges, with a maximum height at 1420 m a.s.l. on Montagne de Boudry (compared to 1080–1180 m a.s.l. during the LGM). North and NE of Neuchâtel, the alpine ice flowed into Val de Travers and Val de Ruz, over Vue des Alpes, passing La Chaux-de-Fond, Le Locle and Pontarlier, to end up some16 km SE of Besançon.

In the study area, the LGM Rhone glacier settled near Solothurn and the ice did not override the border chain except for a few valley floors. However, pre-LGM alpine ice flowed from the Val der Ruz into the Vallon de St Imier which is still covered by pre-LGM till (Bourquin et al., 1946). Further to the east, the glacier penetrated valleys above Biel, then flowing west of Montoz into the upper Birs Valley where it was diluted by local ice (Hantke, 1978). Ice flowed trough the Cluse of Balsthal and filled up the Dünnern valley and also ended up in the Birs Valley. Finally, north of Olten and Aarau, only pre-LGM ice is reported, flowing over various smaller passes to end some 20 km SE of Basel (Hantke, 1978). Further to the east, Rhone ice joined up the piedmont glacier of the western Reuss–Rhein system.

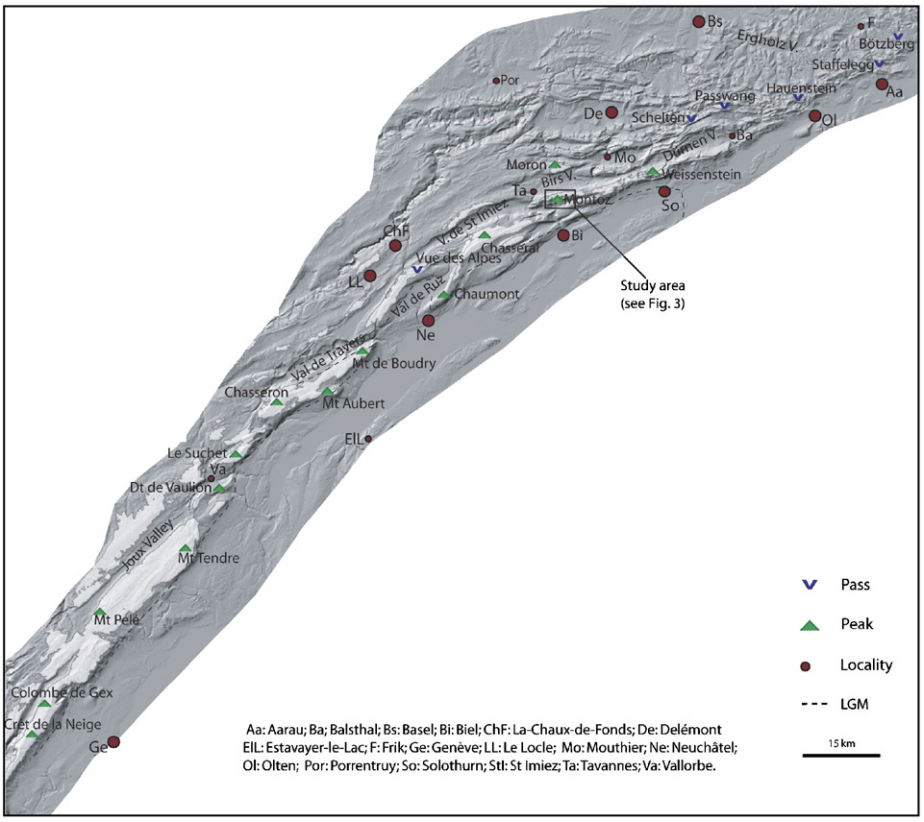

Fig. 2. The morphology of the Jura Mountain chain. White shading indicates areas above 1200 m a.s.l, thus above the generally recognized LGM-ice extent. Vertical exaggeration 3x.

3. Distribution of the erratic boulders

As seen before, the main argument to attribute a moraine or an erratic boulder to a pre-LGM glaciation is its geographic location beyond the generally agreed limits of the LGM (Jäckli, 1962; Schlüchter, 2004). We therefore focus on boulders situated above 1200 m a.s.l. on the border chain, and/or beyond the second anticline. The area between La-Chaux-de-Fond and Le Locle is quite rich in pre-LGM material (Bourquin et al., 1946), which is also found on the French side of the Doubs River, around Pontarlier and as far as the Vallée de la Loue (Hantke, 1978). The easternmost erratic boulder was found in Anwil near Basel (Heim, 1919).

Unfortunately, the modern distribution of erratic boulders is only a relict of the original one. Most of the blocks were destroyed by human activities (Agassiz, 1836; Heim, 1919; De Saussure *in* Aubert, 1986). From those remaining, the majority of the boulders originate from the southern part of the Aar Massif (present Rhone, Fiesch and Aletsch glaciers) but a surprisingly high amount are also attributable to the Mont Blanc Massif, which produces only two relatively small tributary glaciers, Trient and Val d'Entremont, to the Rhone Valley. However, difficulty in distinguishing between Aare and Mont Blanc granites (both are whitish but the latter should be porphyritic and coarser grained) were first pointed out by Heim (1919), and confirmed by Spring (2003). The Penninic napps to the south of the E-W oriented part of the Rhone Valley provide an abundance of metamorphic boulders, including a series of index erratics, mostly gabbros and eclogites from the Zermatt-Saas Zone and Arolla gneisses from the Dent-Blanche napp. The sampled erratic boulders from the Montoz area are pale-greenish rocks, with whitish feldspar–quartz lenses in an oriented matrix composed of muscovite, epidote, and chlorite, with zircon and opaque minerals as accessories. Thin sections have been compared to the descriptions by Aeberhard (1986), Burri et al. (1999) and Abbühl (2004), and according to these, the investigated boulders are attributed to the Arolla gneisses. Kelly et al. (2004) reconstructed the LGM ice surface geometry of the Rhone Valley and suggested that ice from its southern part dominated the Rhone ice flow, pushing the glacier towards the northern valley side. This would explain how boulders from the Zermatt-Saas area have been integrated into the ice, transported to the northern valley side and finally deposited in the eastern Jura Mountains.

4. Cosmogenic dating

4.1. Sampling

The Montoz anticline is situated behind the southern border chain of the Jura Mountains. In the area, pre-LGM

gravels are mapped on both flanks of the anticline (Fig. 3), while no indication for LGM alpine tills have been found so far. However, local tills attributed to the last glacial cycle are covering the valley floors between Montoz and Delémont (Pfirter et al., 1996). Samples were collected from four different erratic boulders distributed on both sides of the anticline. MO-04-01was found on the northern slope, MO-04-02 is located almost on the top, and MO-04-03&-04 lye on the southern slope. Sampling of maximum 2 cm thick rock chips is done with a hammer and chisel (geometric and geographic details are given in Table 1, boulders are shown in Fig. 4). On the rock surfaces, preferential erosion (quartz grains standing 5 mm above other grains) and pitting, with a maximum depth of 1.5 cm, was observed.

4.2. Dating procedures

4.2.1. Cosmogenic radionuclides

The samples were prepared at the Clean Lab of the Institute of Geological Sciences, University of Bern. Grain size was firstly reduced and the sample was homogenized by crushing and sieving; only grains between 0.25 and 0.4 mm were used. Quartz was then isolated physically with a Franz magnetic separator, and then chemically by selective mineral dissolution with hydrochloric and

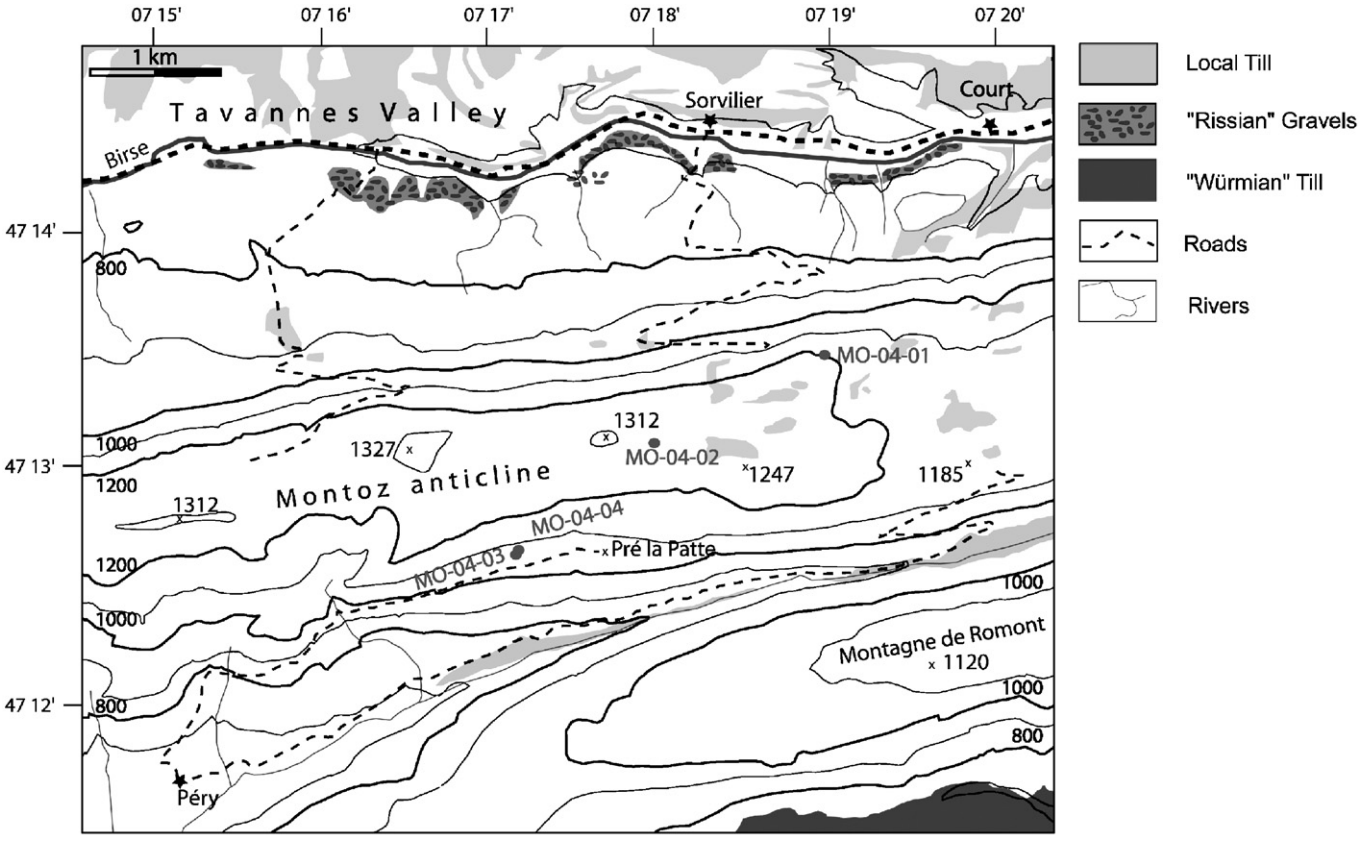

Fig. 3. Sketched map showing sample location on the Montoz anticline. MO-04-01 is located on the northern flank of the anticline, MO-04-02 lies almost on the top, while MO-04-03 and -04 are part of a block field on the southern side. Distribution of glacial deposits modified from Antenen et al. (2004) and Pfirter et al. (1996).

Table 1
Geographic information and boulder geometry of the Montoz samples

Sample	Latitude (°)	Altitude (m a.s.l)	Boulder size ($l \times w \times h$) (m)	Sample height (m)	Surface inclination (inclination; azimut)	Shielding corrections (topo and dip)
MO-04-01	47,225	1200	$2.2 \times 3.8 \times 0.75$	0.5	26; 50	0.9857
MO-04-02	47,218	1260	$1.6 \times 2.2 \times 0.5$	0.5	0; 0	0.9972
MO-04-03	47,209	1050	$2.8 \times 2.2 \times 1.8$	1.8	0; 0	0.9742
MO-04-04	47,210	1060	$8.0 \times 4.5 \times 1.7$	1.3	40; 270	0.9283

Applied corrections are calculated for surrounding topographic shielding and surface geometry.

Fig. 4. Sampled erratic boulders. (A) MO-04-01; (B) surface detail of MO-04-01; (C) MO-04-03, scale is a meter; (D) MO-04-03, scale is a meter.

hydrofluoric acids (Kohl and Nishiizumi, 1992; Biermann et al., 2002). The four samples were treated and measured together with a procedure blank. ^{10}Be was extracted from dissolved pure quartz following the procedure established by Ochs and Ivy-Ochs (1997). Measurements of the beryllium ratio (^{10}Be/^{9}Be) were carried out by accelerator mass spectrometry at the ETH/PSI tandem facility in Zürich-Hönggerberg after Synal et al. (1997).

4.2.2. Cosmogenic noble gas

Neon isotopes were analyzed in ~50 mg sized fractions of the same quartz separates used for radionuclide analyses. The quartz was further crushed to a grain size smaller than 0.1 mm and measured in a non-commercial ultra-high-sensitivity noble gas mass spectrometer, at the Institute of Isotope Geochemistry and Mineral Resources at ETH Zürich (Baur, 1999). Noble gases were extracted in three temperature steps at 600, 800 and 1750 °C, in order to separate the cosmogenic from the non-cosmogenic gas fraction. As derived from the neon three-isotope diagram (Fig. 5), data of all low-temperature steps (600 °C) lie on the atmospheric–cosmogenic mixing line, indicating no nucleogenic neon component. Data from the high-temperature steps (800, 1750 °C) scatter around atmospheric composition and are not considered for age determination. Cosmogenic neon excess (^{21}Ne$_{exc}$) was calculated as excess over air. Uncertainties for the neon data are 1σ and include statistical, sensitivity and mass discrimination errors.

4.2.3. Age calculations

To calculate surface exposure ages, we used the sea level, high latitude production rates of 5.1 and 20.3 atoms g^{-1} SiO_2 yr^{-1}, for ^{10}Be and ^{21}Ne, respectively (Niedermann, 2000; Stone, 2000; Gosse and Stone, 2001). Production rates were scaled to geographic latitude and altitude after Stone (2000). Changes in paleomagnetic intensity and non-dipole effects have not been considered, and sea level changes are not yet integrated. The local production rate was further corrected for topographic shielding and the dip of the samples (between 0 and 40°) after Dunne et al. (1999), and for sample thickness after Gosse and Phillips (2001), using an effective attenuation length of 157 g/cm^2

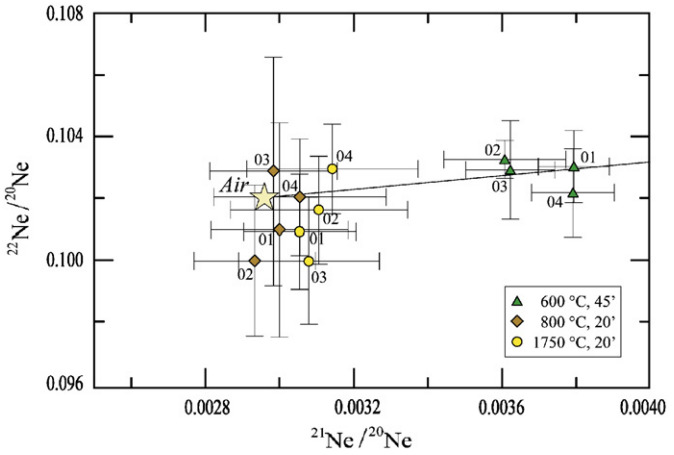

Fig. 5. Neon three-isotope plot of all samples. The line in the panel is the atmospheric–cosmogenic mixing line for quartz, $y = (1.120 \pm 0.021)x + 0.098$, reported by Niedermann (2002).

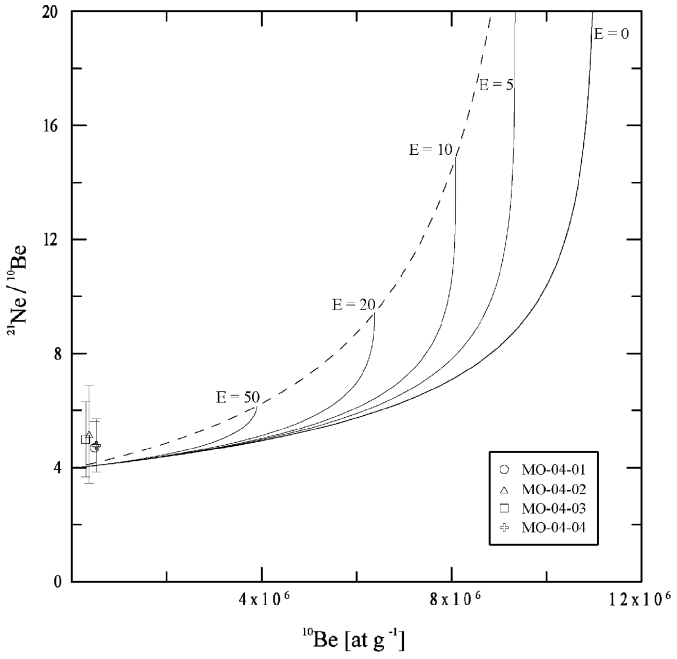

Fig. 6. Two isotope erosion island plot, which allows the determination of long term erosion rates of the sampled surfaces. As our data points fall into the range where all erosion curves converge, we could not determine the rate for the Montoz samples. E = erosion rate in cm/Ma.

and a rock density of 2.65 g/cm^3. Snow corrected ages were obtained by assuming an over-the-year cover of 7 cm of snow (Atlas der Schweiz version 2, by Swisstopo, 2004) with a density of 0.4 g/cm^3. Together with vegetation coverage of 5 cm (density of 0.2 g/cm^3; Tschudi, 2000), we obtained a rock equivalent layer of 1.01 cm. Erosion rate varies in space and time, and is thus the most challenging correction factor of surface exposure dating. Multiple nuclide studies in Switzerland (Ivy-Ochs et al., 2004, 2006a) show that a conservative rate of 3 mm/ka might be a good estimation between steady state erosion and rock-slab split-off for LGM boulders. In order to constrain the erosion rate for the pre-LGM boulders, we plotted the two nuclides on an erosion island plot (Fig. 6) (Graf et al., 1991). Unfortunately, the data points all fall in the convergence curves, we obtained no additional information about the erosion rate. As seen in Fig. 7, the ^{10}Be and ^{21}Ne concentrations from the four boulders show excellent agreement and support the hypothesis of continuous single-stage exposure. Therefore we present our ages as apparent ages, as well as corrected for conservative erosion rates of 1 ± 0.5 and 3 ± 0.5 mm/ka.

4.3. Results

Radionuclide ages are given in Table 2 and noble gas ages in Table 3. For the two larger boulders, we obtained apparent exposure ages of 99 ± 3 ka (^{10}Be) and 112 ± 11 ka (^{21}Ne) for MO-04-01 and 107 ± 6 ka (^{10}Be) and 123 ± 12 ka (^{21}Ne) for MO-04-04. We reproduce the same age as Ivy-Ochs obtained on a different sample of boulder MO-04-01 at the ETH/PSI laboratory (Ivy-Ochs et al., 2006b). The two smaller boulders are considerably younger with apparent ages of 75 ± 8 ka (^{10}Be) and 94 ± 15 ka (^{21}Ne) for MO-04-02 and 60 ± 4 ka (^{10}Be) and 73 ± 10 ka (^{21}Ne) for MO-04-03. By applying a conservative erosion rate of 3 ± 0.5 mm/ka, the radionuclide ages increase to 143 ± 17 ka (^{10}Be) and 124 ± 12 ka (^{21}Ne) for MO-01-04; 163 ± 21 ka (^{10}Be) and 138 ± 13 ka for MO-04-04; 98 ± 11 ka (^{10}Be) and 103 ± 17 ka (^{21}Ne) for MO-04-02; and 74 ± 6 ka (^{10}Be) and 80 ± 11 ka (^{21}Ne) for MO-04-03.

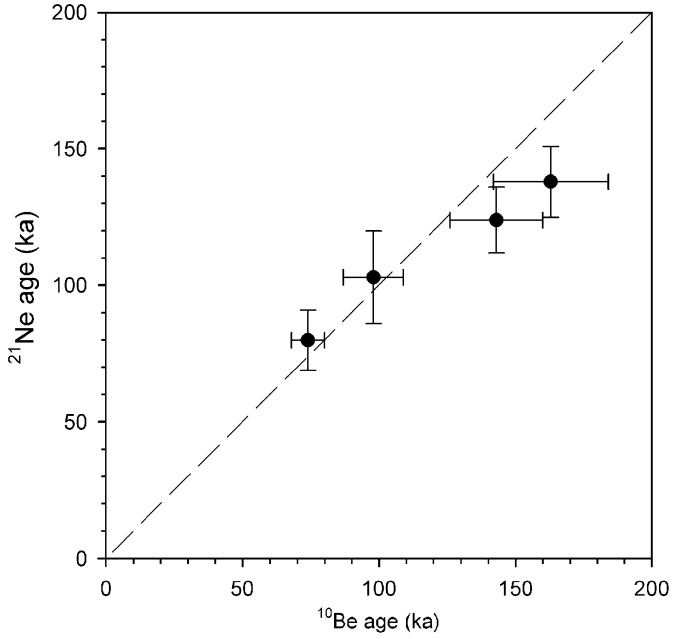

Fig. 7. Two-isotope plot, showing the good correlation between ^{21}Ne and ^{10}Be ages within 1σ errors. However, ^{21}Ne ages are systematically slightly older.

As the boulders are all of the same lithology on a quite narrow location, we do not expect them to have been deposited by different glacial advances. However, a purely

down wasting ice body cannot explain the age differences of the four boulders because, if so, we would expect the more elevated one to be the oldest. Although boulder MO-04-02 lies almost on the summit of the anticline, its age is quite young.

In surface exposure dating, only pre-exposure would explain age overestimates (ruled out in this study by applying both noble gases and radionuclides), while several processes can lead to younger ages. One of them would be post-depositional rotation of a boulder. In fact, based only on field evidence, we could not exclude post depositional movement of the tabular shaped bloc MO-04-02, e.g. by farming activities. Assuming that the sampled top surface was once the boulders' bottom, we recalculate the production rate for a depth of 50 cm, and the obtained ^{10}Be apparent age is 172 ± 10 ka. As agricultural activity began in the Neolithic (Brombacher, 1997), overturning of the boulder by farming could only explain age differences of a few thousand years. Boulders MO-04-03 and MO-04-04 are part of a small block filed on a 24° slope, the latter about 10 m above the first. Soil creep could have slid the smaller rock for some meters, but rotation would likely induce more dynamic movements toward the valley. Alternatively, a younger age of a boulder within a sample set can be explained by its post-depositional coverage with sediment causing a decrease of the production rate (Putkonen and Swanson, 2003). We exclude coverage of solely MO-04-03 because of the above described sample site characteristics. However it can be reasonably assumed that 0.5 m tall boulder MO-04-02 was buried under a sediment layer after glacier retreat. Finally, as most of the cosmogenic nuclides accumulate in the upper 20 cm, periodical split-off of rock slabs sets the clock back for thousands of years. As shown in Fig. 4C, a bit on the upper left part of boulder MO-04-03 seems to be missing. However this mechanism can be excluded for MO-04-02 because of its regular and flat top surface.

For the reasons explained above, our larger blocks certainly better represent deposition time because we avoid substantial post-depositional coverage. In addition, it has been statistically shown by Putkonen and Swanson (2003) that in many cases older ages from a data set are more representative of the true deposition age than younger ones. According to this, the boulders were deposited on the Montoz anticline between 126 and 184 ka, a time span corresponding to Marine Isotope Stage (MIS) 6.

Table 2
Accelerator mass spectrometry results of the Montoz samples and resulting ages

Sample	^{10}Be (10^6 atoms/g)	^{10}Be apparent age (ka)	^{10}Be age (kyr) $\varepsilon = 1$ mm/ka	^{10}Be age (kyr) $\varepsilon = 3$ mm/ka
MO-04-01	1.35 ± 0.04	99 ± 3	111 ± 11	143 ± 17
MO-04-02	1.09 ± 0.11	75 ± 8	82 ± 9	98 ± 11
MO-04-03	0.73 ± 0.05	60 ± 4	65 ± 5	74 ± 6
MO-04-04	1.23 ± 0.06	107 ± 6	121 ± 13	163 ± 21

Apparent ages are corrected for thickness and shielding, the erosion corrected ages also contain corrections for snow and vegetation cover, see text for details. Errors are given with 1σ uncertainties, excluding systematic production rate error.

5. Discussion

How then does the timing of a MIS-6 glaciation presented in this work relate to the events in the Swiss Midlands? Beside the maximum of the last glaciation dated near Solothurn by Ivy-Ochs et al. (2004), some evidence for pre-LGM glaciations have been documented in the Swiss Midlands, joining the complexity of pollen profiles e.g. Gondiswil (Wegmüller, 1992), Füramoos in southern

Table 3
Neon data and apparent ages

Sample	Heating temperature (°C); time (min)	^{20}Ne (10^9 atoms/g)	^{21}Ne/^{20}Ne (10^{-3})	^{22}Ne/^{20}Ne	^{21}Ne$_{exc}$ (10^6 atoms/g)	^{21}Ne age (apparent, ka)	^{21}Ne age ($\varepsilon = 1$ mm/ka)	^{21}Ne age ($\varepsilon = 3$ mm/ka)
MO-04-01	600; 45	7.579 ± 0.1209	3.79 ± 0.10	0.1030 ± 0.0012	6.34 ± 1.22	112 ± 11	114 ± 11	124 ± 12
	800; 20	1.568 ± 0.0202	3.00 ± 0.18	0.1010 ± 0.0035	0.07 ± 0.36			
	1750; 20	2.881 ± 0.0626	3.06 ± 0.15	0.1009 ± 0.0019	0.28 ± 0.66			
MO-04-02	600; 45	8.68 ± 0.10	3.61 ± 0.16	0.1033 ± 0.0006	5.64 ± 1.78	94 ± 15	98 ± 16	103 ± 17
	800; 20	1.91 ± 0.0582	2.93 ± 0.16	0.1000 ± 0.0024	0.00 ± 0.00			
	1750; 20	2.953 ± 0.0315	3.11 ± 0.24	0.1016 ± 0.0017	0.44 ± 0.80			
MO-04-03	600; 45	5.475 ± 0.0746	3.62 ± 0.12	0.1029 ± 0.0016	3.64 ± 0.94	73 ± 10	74 ± 10	80 ± 11
	800; 20	1.258 ± 0.0332	2.99 ± 0.17	0.1029 ± 0.0037	0.03 ± 0.34			
	1750; 20	2.10 ± 0.0297	3.08 ± 0.19	0.1000 ± 0.0021	0.26 ± 0.50			
MO-04-04	600; 45	7.047 ± 0.0869	3.79 ± 0.11	0.1022 ± 0.0014	5.87 ± 1.12	123 ± 12	126 ± 12	138 ± 13
	800; 20	1.193 ± 0.0358	3.06 ± 0.23	0.1020 ± 0.0019	0.12 ± 0.40			
	1750; 20	1.858 ± 0.0641	3.14 ± 0.23	0.1030 ± 0.0015	0.34 ± 0.66			

Uncertainties for the neon data are 1σ and include statistical, sensitivity and mass discrimination errors.

Germany (Müller et al., 2003), Les Echets near Lyon (de Beaulieu and Reille, 1984) and Grande Pile in the Vosges (de Beaulieu and Reille, 1992). For example, indices for early late Pleistocene glaciations, i.e. MIS-5d/b and MIS-4, have been dated at Gossau (near Zürich), Finsterhennen (South of Lake Neuchâtel), and Thalgut (S of Bern) (Preusser et al., 2003, 2007; Preusser, 2004; Preusser and Schlüchter, 2004), as well as from Grandson (Badoux, 1995) and Les Tuilleries (Jayet and Portmann, 1960, 1966).

However, only few pre-Eemian sediment records have been found until now. The Thalgut gravel pit mentioned above presents a very complete sediment succession described in detail in Schlüchter (1989a, b). The lowermost part of the profile is formed by a till followed concordantly by lacustrine silts (Jaberg Seetone). These lacustrine silts were correlated to the Holsteinian period by Welten (1982, 1989), based on the pollen assemblage (*Pterocarya* and domiance of Fagus). They are overlain by a prograding delta, progressively more glacigenic and a coarsening-upward sequence, which is itself conformably overlain by a waterlain till and a 4 m thick sandy–silty varve succession. These older sediments are cut by a broad erosional unconformity, that was preceded by an important pedogenic event. Above the erosion surface lies up to 30 m of the Kirchberg gravels delta, its fore-sets dipping towards the present-day Aare River. The presence of a glacier is inferred from this different hydrological control, even if the gravels and sands contain only local reworked material. The concordantly overlying Thalgut Seetone, also dipping toward the present day river, are interpreted as basin accumulation during the Last Interglacial (Welten, 1982, 1988). These silts are followed by up to 30 m of the Upper Münsingen gravels (braided river system), divided into two units by an erosional surface. The lower unit has been dated and correlated with MIS-5d (Preusser and Schlüchter, 2004). The upper unit is overlain by a 6 m thick LGM lodgement till. If the Thalgut Seetone are interglacial MIS-5e in age, the Kirchdorf gravels under these silts have most probably been deposited at the same time as the Montoz erratic boulders, or slightly later, before climate amelioration led to re-vegetation and deposition of the Eemian silts in a lacustrine environment.

The second long sediment record discussed here was drilled near Meikirch, north of Bern. The laminated sand and silts of the Meikirch complex represent three warm periods and four stadial periods, preceded and followed by sediments deposited during full glacial times. Preusser et al. (2005) have completely re-interpreted the pollen analysis and partly re-interpreted the sediment analyses presented in Welten (1982, 1989). They attribute the Meikirch complex to the MIS-7, overlain by 40 m of fluvio–glacial and glacial sediments, showing at least two glaciations. Three samples have been taken from silty to sandy layers between 19 and 28 m. The obtained OSL ages are between 186 and 206 ka, indicating a pre-Eemian glacial advance in this area.

6. Conclusions

In this study we successfully applied Surface Exposure Dating to older erratic boulders in the mid-latitudes. Both radionuclides and noble gases results are in good agreement and encouraging for further studies. The dated boulders from the Montoz anticline show pre-Eemian ages between 126 and 184 ka, and we propose here a correlation with MIS-6. This implies (i) the larger than LGM glaciation responsible for the deposition of the erratic boulders on the Montoz anticline correlates most probably to the Rissian proposed by Penck and Brückner (1901–1909), (ii) the early late Pleistocene glaciations (i.e. MIS 5d, 5b and 4) were of less extent than both MIS-6 glaciation and LGM, (iii) such an important ice advance and associated high erosive activity can easily explain the scarcity of pre-Eemian sediment records in the narrow Swiss Midlands.

Acknowledgements

We thank F. Preusser, P. Häuselmann and C. Buoncristiani for critical reviews, D. Ricke-Zapp for GIS- Support, as well as the ETH-PSI facility at Zürich-Hönggenberg for Technical support. The Zurich AMS facility is jointly operated by the Swiss Federal Institute of Technology, Zurich and by Paul Scherrer Institute, Villigen, Switzerland. This work was funded by Swiss National Research Grant no. 200020-105220/1.

References

Abbühl, L.M., 2004. A zero-exposure-time experiment on a sub-recent erratic: the problem of pre-exposure in dating with cosmogenic nuclides. Unpublished Diploma Thesis, ETHZ, Switzerland.

Aeberhard, T., 1986. Verzeichnis der geschützten geologischen Objekte des Kantons Bern. Naturschutzinspektorat des Kantons Bern, Bericht.

Agassiz, L., 1836. Distribution des blocs erratiques sur les pentes du Jura. Bulletin de la Société Geologique de France 1, 7.

Agassiz, L., 1843. Le Jura a eu ses glaciers propres. Actes Société Helvétique de Sciences naturelles, 28è session, Lausanne.

Antenen, M., Kellerhals, P., Tröhler, B., 2004. Geologischer Atlas der Schweiz, 1:25'000 Blatt 109 „Büren a. d. Aare" und Erläuterungen. Landeshydrologie und –geologie, Bern.

Arn, R., Aubert, D., 1984. Les formations quaternaires de l'Orbe et du Nozon, au pied du Jura. Bulletin de Géologie (Lausanne) 275, 17–42.

Atlas der S., 2004. Version 2.0, Bundesamt für Landestopografie, Wabern.

Aubert, D., 1938. Les glaciers quaternaires d'un bassin fermé: la vallée de Joux (Canton de Vaud). Bulletin des laboratoires de Géologie, Géographie physique, Mineralogie et Paléontologie de l'Université de Lausanne 62, 1–14.

Aubert, D., 1965. Calotte glaciaire et morphologie jurassienne. Eclogae Geologicae Helveticae 58, 555–578.

Aubert, D., 1986. La récurrence des glaciers jurassiens entre la Venoge et l'Aubonne. Bulletin de Géologie (Lausanne) 285, 21–46.

Badoux, H., 1995. Le glacier du Rhône au Pléistocène. Bulletin des laboratoires de Géologie, Géographie physiques, Mineralogie et Paléontologie de l'Université de Lausanne 329, 245–292.

Baur, H., 1999. A noble-gas mass spectrometer compressor source with two orders of magnitude improvement in sensitivity. EOS Transactions, AGU Fall Meeting 80 (46 Suppl.).

Biermann, P.R., Caffee, M.W., Davis, P.T., Marsella, K., Pavich M., Colgan, P., Mickelson, D., Larsen, J., 2002. Rates and timing of earth surfaces processes from in-situ produced cosmogenic Be-10. In: Grew, E.S. (Ed.), Beryllium: Mineralogy, Petrology and Geochemistry. Reviews in Mineralogy and Geochemistry 50, pp. 147–205.

Bourquin, P., Suter, H., Fallot, P., 1946. Atlas Geologique de la Suisse, 1:25'000 Feuilles 114 "Biaufond", 115 "Les Bois", 116 "La Ferrière", 117 "St-Imier", et Notices Explicatives. Service hydrologique et géologique national, Berne.

Brombacher, C., 1997. Archeobotanical investigations of late neolithic lakeshore settlements (lake Biel, Switzerland). Vegetation History and Archeobotany 6, 167–186.

Buoncristiani, J.F., Campy, M., 2004a. Expansion and retreat of the Jura ice sheet (France) during the last glacial maximum. Sedimentary Geology 165, 253–264.

Buoncristiani, J.F., Campy, M., 2004b. The paleogeography of the two last glacial episodes in France: the Alps and Jura. In: Ehlers, J., Gibbard, P.L. (Eds.), Quaternary Glaciations—Extent and Chronology. Part I: Europe. Elsevier B.V., Amsterdam, pp. 101–112, 474pp.

Burri, M., Dal Piaz, G.V., Della Valle, G., Gouffon, Y., Germani, A., 1999. Geologischer Atlas der Schweiz 1:25'000, Blatt 1346, Chanrion, und Erläuterungen. Landeshydrologie und –geologie, Wabern, Schweiz.

Campy, M., 1992. Palaeogeographical relationship between Alpine and Jura glaciers during the two last Pleistocene glaciations. Palaeogeography, Palaeoclimatology, Palaeoecology 93, 1–12.

Campy, M., Arn, R., 1991. The Jura glaciers: palaeogeography in the Würmian circum-Alpine zone. Boreas 20, 17–27.

De Beaulieu, J.-L., Reille, M., 1984. A long Upper Pleistocene pollen record from les Echets near Lyon, France. Boreas 13, 111–132.

De Beaulieu, J.-L., Reille, M., 1992. The last climatic cycles at La Grande Pile (Vosgues, France): a new pollen profile. Quaternary Science Reviews 11, 431–438.

Dunne, J., Elmore, D., Muzikar, P., 1999. Scaling factors for the rates of production of cosmogenic nuclides for geometric shielding and attenuation at depth on sloped surfaces. Geomorphology 27, 3–11.

Gosse, J.C., Phillips, F.M., 2001. Terrestrial in situ cosmogenic nuclides; theory and application. Quaternary Science Reviews 20, 1275–1560.

Gosse, J.C., Stone, J.O., 2001. Terrestrial cosmogenic nuclide methods passing milestones toward paleo-altimetry. EOS (Transactions, American Geophysical Union), 82, 86, 89.

Graf, T., Kohl, C.P., Marti, K., Nishiizumi, K., 1991. Cosmic ray produced neon in Antarctic rocks. Geophysical Research Letters 18, 203–206.

Heiri, O., Millet, L., 2005. Reconstruction of Late Glacial summer temperatures from chironomid assemblages in Lac Lautrey (Jura, France). Journal of Quaternary Sciences 20, 33–44.

Hantke, R., 1978. Eiszeitalter, Band I: Die jüngste Erdgeschichte der Schweiz und ihrer Nachbargebiete. Ott Verlag AG Thun.

Heim, A., 1919. Geologie der Schweiz. 2 Bände in 4 Teilen. C.H. Tauchnitz, Leipzig, 704 und 1018pp.

Ivy-Ochs, S., Schäfer, J., Kubik, P.W., Synal, H.-A., Schlüchter, C., 2004. Timing of deglaciation on the northern Alpine foreland (Switzerland). Eclogae Geologicae Helveticae 97, 47–55.

Ivy-Ochs, S., Kerschner, H., Kubik, P.W., Schlüchter, C., 2006a. Glacier response in the European Alps to Heinrich Event 1 cooling: the Gschnitz stadial. Journal of Quaternary Science 21, 115–130.

Ivy-Ochs, S., Kerschner, H., Reuther, A., Maisch, M., Sailer, R., Schaefer, J., Kubik, P.W., Synal, H.-A., Schlüchter, C., 2006b. The timing of glacier advances in the northern European Alps based on surface exposure dating with cosmogenic 10Be, 26Al, 36Cl, and 21Ne. In: Siame, L.L., Bourles, D.L., Brown, E.T. (Eds.), In Situ Cosmogenic Nuclides and their Applications in Earth Sciences. GSA Special Paper 415, pp. 43–60.

Jäckli, H., 1962. Die Vergletscherung der Schweiz im Würmmaximum. Eclogae Geologicae Helveticae 55, 185–294.

Jayet, A., Portmann, J.-P., 1960. Deux gisement interglaciaires nouveaux aux environs d'Yverdon (Vaud, Suisse). Eclogae Geologicae Helveticae 53, 640–645.

Jayet, A., Portmann, J.-P., 1966. Sur la presence de moraines rissiennes profondes dans le gisement quaternaire des Tuilleries près d'Yverdon (Vaud, Suisse). Eclogae Geologicae Helveticae 59, 960–964.

Kelly, M., Buoncristiani, J., Schlüchter, C., 2004. A reconstruction of the last glacial maximum (LGM) ice-surface geometry in the western Swiss Alps and contiguous Alpine regions in Italy and France. Eclogae Geologicae Helvetiae 97, 57–75.

Kohl, C.P., Nishiizumi, K., 1992. Chemical isolation of quartz for measurement of in situ produced cosmogenic nuclides. Geochimica et Cosmochimica Acta 56, 3585–3587.

Labhart, T., 1992. Geologie der Schweiz. Ott Verlag, Thun, 211pp.

Moscariello, A., Pugin, A., Wildi, W., Beck, C., Chapron, E., De Batist, M., Girardclos, S., Ivy-Ochs, S., Rachoud-Schneider, A.-M., Signer, C., Van Cauwenberghe, T., 1998. Déglaciation würmienne dans des conditions lacustres à la terminaison occidentale du basin lémanique (Suisse occidentale et France). Eclogae Geologicae Helveticae 91, 185–201.

Muller, U.C., Pross, J.O., Bibus, E., 2003. Vegetation response to rapid climate change in central europe during the past 140,000 yr based on evidence from the Furamoos pollen record. Quaternary Research 59, 235–245.

Niedermann, S., 2000. The ^{21}Ne production rate in quartz revisited. Earth and Planetary Science Letters 183, 361–364.

Niedermann, S., 2002. Cosmic-ray-produced noble gases in terrestrial rocks: dating tools for surface processes. In: Porcelli, D., Ballentine, C.J., Wieler, R. (Eds.), Noble gases in geochemistry and cosmochemistry. Reviews in Mineralogy and Geochemistry 47, pp. 731–784.

Nussbaum, F., Gygax, F., 1935. Zur Ausdehnung des risseiszeitlichen Rhonegletschers im französischen Jura. Eclogae Geologicae Helveticae 28, 659–665.

Oberholzer, P., 2000. Reconstructing paleoclimate and landscape history in Antarctica and Tibet with cosmogenic nuclides. Dissertation ETH-15472, Zürich, Switzerland.

Oberholzer, P., Baroni, C., Schäfer, J., Orombelli, G., Ivy-Ochs, S., Kubik, P., Baur, H., Wieler, R., 2003. Limited Pliocene/Pleistocene glaciation in Deep Freeze Range, northern Victoria Land, Antarctica, derived from in situ cosmogenic nuclides. Antarctic Sciences 15, 493–502.

Ochs, M., Ivy-Ochs, S., 1997. The chemical behavior of Be, Fe, Ca and Mg during AMS target preparation from terrestrial silicates modeled with chemical speciation calculations. Nuclear Instruments and Methods in Physics Research B 123, 235–240.

Penck, A., Brückner, E., 1901–1909. Die Alpen im Eiszeitalter. Tauchnitz, Leipzig, 1199pp.

Pfirter, U., Antenen, M., Burkhalter, R.M., Gürler, B., Krebs, D., 1996. Geologischer Atals der Schweiz, Blatt 96 „Moutier" und Erläuterungen. Landeshydrologie und –geologie, Bern.

Preusser, F., 2004. Towards a chronology of the Late Pleistocene in the northern Alpine Foreland. Boreas 33, 195–210.

Preusser, F., Schlüchter, C., 2004. Dates from an important early Late Pleistocene ice advance in the Aare valley, Switzerland. Eclogae Geologicae Helveticae 97, 245–253.

Preusser, F., Gehy, M.A., Schlüchter, C., 2003. Timing of Late Pleistocene climate change in lowland Switzerland. Quaternary Science Reviews 22, 1435–1445.

Preusser, F., Drescher-Schneider, R., Fiebig, M., Schlüchter, C., 2005. Reinterpretation of the Meikirch pollen record, Swiss Alpine Foreland, and implications for Middle Pleistocene chronostratigraphy. Journal of Quaternary Science 20, 1–14.

Preusser, F., Blei, A., Graf, H.-R., Schlüchter, C., 2007. Luminescence dating of Würmian (Weichselian) proglacial sediments from Switzerland; methodological aspects and stratigraphical conclusions. Boreas, in press.

Putkonen, J., Swanson, T., 2003. Accuracy of cosmogenic ages for moraines. Quaternary Research 59, 255–261.

Schäfer, J., Tschuddi, S., Zhao, Z., Wu, Z., Ivy-Ochs, S., Wieler, R., Baur, H., Kubik, P., Schlüchter, C., 2002. The limited influence of glaciation

in Tibet on global climate over the past 170 000 yr. Earth and Planetary Science Letters 194, 287–297.

Schlüchter, C., 1989a. The most complete Quaternary record of the Swiss Alpine foreland. Palaeogeography, Palaeoclimatology, Palaeoecology 72, 141–146.

Schlüchter, C., 1989b. Thalgut. Ein umfassendes eiszeitstratigraphisches Referenzprofil im nördlichen Alpenvorland. Eclogae Geologicae Helveticae 82, 277–284.

Schlüchter, C., 2004. The Swiss glacial record—a schematic summary. In: Ehlers, J., Gibbard, P.L. (Eds.), Quaternary Glaciations—Extent and Chronology. Part I: Europe. Elsevier B.V., Amsterdam, pp. 413–418, 474pp.

Schlüchter, C., Kelly, M., 2001. Das Eiszeitalter in der Schweiz. Stiftung Landschaft und Kies, Uttigen.

Spring, J., 2003. Provenance des blocs erratiques granitique du glacier du Rhône. Unpublished Diploma Thesis, University of Neuchâtel, Switzerland.

Stone, J.O., 2000. Air pressure and cosmogenic isotope production. Journal of Geophysical Research 105, 23753–23759.

Synal, H.-A., Bonani, G., Döbeli, M., Ender, R.M., Gartenmann, P., Kubik, P.W., Schnabel, C., Sutter, M., 1997. Status Report of the PSI/ETH AMS facility. Nuclear Instruments and Methods in Physics Research B 123, 62–68.

Trümpy, R., 1980. Geology of Switzerland, Part A and B. Wepf & Co. Publishers, Basel, 104 and 334pp.

Tschudi, S., 2000. Surface exposure dating: a geologist's view with examples from both hemispheres. Dissertation, Universtiy of Bern.

Vannières, B., Bossuet, G., Walter-Simonnet, A-V., Ruffaldi, P., Addatte, T., Rossy, M., Magny, M., 2004. High-resolution recore of environmental changes and tephrochronological markers of the Last Glacial-Holocene transition at Lake Lautrey (Jura, France). Journal of Quaternary Sciences 19, 797–808.

Vuille, A., 1965. Extension du glacier du Rhône dans les montagnes neuchâteloises à l'époque rissienne. Bulletin de la société neuchâteloise de géographie, tome LIII, Fasc, 1–13, 45–66.

Wegmüller, S., 1992. Vegetationsgeschichtliche und stratigraphische Untersuchungen an Schieferkohles des nördlichen Alpenvorlandes. Denkschreiben der Schweizerischen Akademie der Naturwissenschaften 102, 1–82, 3 Profile.

Welten, M., 1982. Pollenanalytische Untersuchungen im Jüngeren Quartär des nördlichen Alpenvorlandes der Schweiz. Beiträge zur Geologischen Karte der Schweiz, NF 156, 1–174, mit Diagrammheft.

Welten, M., 1988. Neue pollenanalytische Ergebnisse über das jüngere Quartär des nördlichen Alpenvorlandes der Schweiz (Mittel und Jungpleistozän). Beiträge zur Geolgosichen Karte der Schweiz, NF 162, 1–40.